Equation of state of shock-compressed liquids: Carbon dioxide and air

W. J. Nellis, A. C. Mitchell, F. H. Ree, M. Ross, N. C. Holmes, R. J. Trainor,[a] and D. J. Erskine
Lawrence Livermore National Laboratory, University of California, Livermore, California 94550

(Received 13 May 1991; accepted 17 June 1991)

Equation-of-state data were measured for liquid carbon dioxide and air shock-compressed to pressures in the range 28–71 GPa (280–710 kbar) using a two-stage light-gas gun. The experimental methods are described. The data indicate that shock-compressed liquid CO_2 decomposes at pressures above 34 GPa. Liquid air dissociates above a comparable shock pressure, as does liquid nitrogen. Theoretical intermolecular potentials are derived for CO_2 from the data. The calculated shock temperature for the onset of CO_2 decomposition is 4500 K at a volume of 17 cm^3/mol.

I. INTRODUCTION

Shock compression of molecular liquids produces high densities and temperatures which induce a variety of phenomena. For example, carbonaceous molecules, such as CO, decompose and react to form mixtures of chemical species.[1] Diatomic molecules, such as N_2 and O_2, dissociate.[2,3] The properties of CO_2, N_2, and O_2 and their mixtures are of interest because of their presence in reacted explosives. In addition species containing C, O, and N are present at high densities and temperature in the interiors of the giant planets Uranus and Neptune. Experimental equation-of-state data are required to develop reliable theoretical descriptions of molecular systems at high pressures and temperatures. Such descriptions are useful for developing models of planetary interiors and reacted explosives, for example.

Carbon dioxide has been single-shocked to 63 GPa (630 kbar) using solid specimens.[4] Liquid specimens were single-shocked to 29 GPa and double-shocked to 56 GPa.[5] Solid specimens have been compressed statically as high as 51 GPa.[6–8] All these data are in the range of stability of the CO_2 molecule. In this paper we report equation-of-state results for liquid CO_2 single-shocked in the range 28–71 GPa. The purpose was to look for the onset of molecular decomposition at higher pressures and temperatures than achieved previously. Equimolar mixtures of liquid N_2 and O_2 were single-shocked to 24 GPa and double-shocked to 66 GPa.[9] We report herein results for liquid air single-shocked in the range 28–69 GPa, which is within the range of dissociation of both N_2 and O_2.[2,3,10–12] The data reported here indicate that shocked liquid CO_2 begins to decompose above 34 GPa and liquid air dissociates above a comparable shock pressure.

II. EXPERIMENT

Equation-of-state data were measured using a method based on the Rankine–Hugoniot equations, which conserve mass, momentum, and energy across the front of a shock wave. The equations are

$$P - P_0 = \rho_0 (u_s - u_0)(u_p - u_0), \tag{1}$$

$$V = V_0 [1 - (u_p - u_0)/(u_s - u_0)], \tag{2}$$

$$E - E_0 = 0.5(P + P_0)(V - V_0), \tag{3}$$

where P_0, ρ_0, E_0, and u_0 are, respectively, the initial pressure, density, specific internal energy, and mass velocity of the material ahead of the shock front; $V_0 = 1/\rho_0$ is the initial specific volume; P, V, and E are, respectively, the final shock pressure, specific volume, and specific internal energy; u_s is the velocity of the shock wave; and u_p is the mass velocity of the material behind the shock front.

The experiments involve measurements of the velocity of impact u_I of a metal plate and of the velocity of the shock wave u_s induced in a specimen.[13–15] The plate, of Ta or Al alloy 1100 in these experiments, is accelerated to several km/s by a two-stage light-gas gun. Impact velocity is measured by flash x-radiography and shock velocity is measured with electrical shock-arrival-time detectors.

Liquid specimens were prepared by condensing high-purity gaseous CO_2 or dry air (78.1% N_2, 21.0% O_2, and 0.9% Ar) into a precooled specimen holder. The specimen holder is positioned on the axis of the gun in the evacuated target chamber. For the CO_2 experiments the initial specimen conditions were chosen to be essentially the same as those used by Schott.[5] The Al specimen holder was controlled at a temperature of ~218 K by control of the flow of cold N_2 gas.[16] Initial specimen temperature was measured with a calibrated Pt resistance thermometer. The condensed specimen was pressurized to ~7 bar with CO_2 gas to achieve the liquid phase. Initial specimen pressure was measured with a capacitance manometer. To obtain minimal distortion of the impact wall or base plate of the liquid specimen holder, caused by the 7 bar differential pressure across it, a 3 mm thick Al alloy 1100 base plate was used. The electrical shock detectors were positioned on radii of 5.0 and 8.5 mm with a detector on axis, as previously.[14] The separation of the two planes on which the detectors are positioned was 2.0 mm. Metal impactor plates were 25 mm in diameter. For the liquid–air experiments liquid N_2 was used as the coolant.[14] Initial specimen temperature was taken to be the temperature on the nitrogen saturation curve at the measured barometric pressure. The Al alloy 1100 base plate was 2 mm thick. For CO_2 and air initial specimen pressures were set ~900 and 50 Torr, respectively, above saturation pressure to suppress boiling and bubbles in the specimens. Initial

[a] Present address: Los Alamos National Laboratory, Los Alamos, New Mexico 87545.

 0021-9606/91/195268-05$03.00

TABLE I. Coefficients C and S, where $u_s = C + Su_p$, for the shock-wave equations of state of Al and Ta, including coefficients of Al corrected for the 77 K initial temperature of the liquid air experiments.

Metal	T_0(K)	C(cm/μs)	S
Al	300	0.5386	1.339
Al	77	0.5420	1.334
Ta	300	0.3291	1.308

specimen density was taken to be that of the published saturation curve at initial specimen temperature for CO_2,[17] and air.[18]

Shock pressure, density, and specific internal energy are derived from the measured impactor and shock velocities and initial specimen density by the shock-impedance-matching process and the Rankine–Hugoniot Eqs. (1)–(3). The shock-wave equations of state of the Al (Ref. 19) and Ta (Refs. 19 and 20) impactor plates and the cold-Al (Ref. 14) base plate of the specimen holder, which were used in the shock-impedance-matching process,[14,15] are listed in Table I. These shock-wave equations of state are represented by a linear relation between shock and mass velocity: $u_s = C + Su_p$.

III. EXPERIMENTAL RESULTS

The single-shock equation-of-state data of liquid CO_2 and air are listed in Table II. Shock velocity vs mass velocity are plotted for CO_2 in Fig. 1. The CO_2 data of Schott[5] are also plotted in Fig. 1. The two data sets agree in the overlap region near shock velocity of 7 km/s. Our data point at 28 GPa is in good agreement with the linear fit to the $u_s - u_p$ data of Schott in the u_p range 2.0–3.6 km/s: $u_s = C + Su_p$, where $C = 1.69$ km/s and $S = 1.40$. The data for CO_2 plotted in Fig. 1 show a change in slope at $u_p = 4$ km/s, which corresponds to a shock pressure of 34 GPa. Such a slope change indicates the onset of chemical decomposition, as observed in CS_2,[21] CO,[1] and N_2,[2,15] for example.

Shock velocity vs mass velocity are plotted for liquid air in Fig. 2. For comparison the corresponding fit to the data of liquid nitrogen,[15] which composes 78% of air, is also plotted in Fig. 2. The $u_s - u_p$ data of air in Fig. 2 are quite similar to those of nitrogen and suggest that the nitrogen molecules in air dissociate above about 30 GPa, as in pure nitrogen.[14] Dissociation occurs at a similar shock pressure in liquid oxygen.[3]

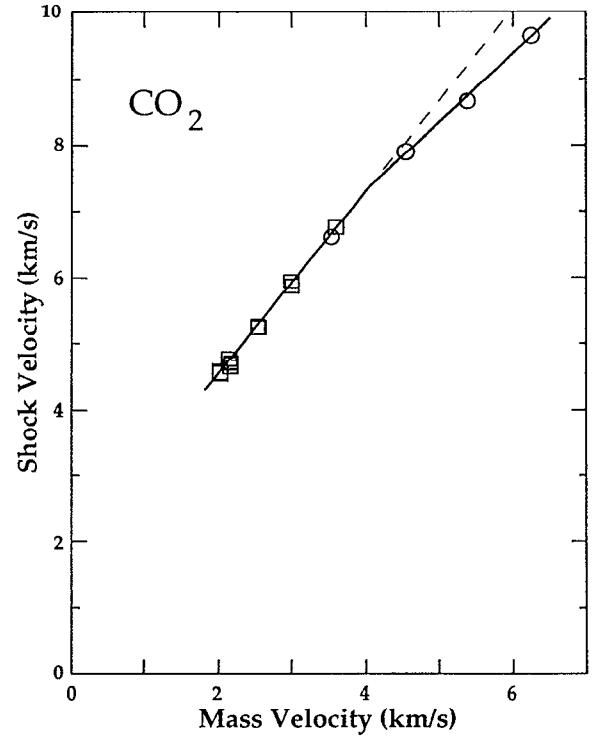

FIG. 1. Shock velocity vs mass velocity for liquid carbon dioxide. Circles are this work; squares are from Ref. 5. Dashed line is extrapolation of linear fit to data of Ref. 5.

IV. THEORETICAL CALCULATIONS FOR CO_2

As described in Sec. III, the experimental data for CO_2 indicate shock-induced dissociation at pressures above ~34 GPa. This phenomena can be characterized with a theoretical calculation using the Gibb's free energy $G(P,T,\{n_i\})$, which includes both CO_2 and its dissociation products. The calculations presented here utilize five gaseous species (CO_2,CO,O_2,O,O_3) and three condensed forms of carbon (liquid, graphite, and diamond). The condensed phases are

TABLE II. Hugoniot data for liquid CO_2 and air. The initial densities of the Al (alloy 1100) impactors were 2.708 and 2.716 g/cm^3 for the CO_2 and air experiments, respectively. The initial density of the Al (alloy 1100) base plates were 2.718 and 2.747 g/cm^3 for the CO_2 and air experiments, respectively, with thermal contraction taken into account. The initial density of the Ta impactors was 16.66 g/cm^3. The average initial molar volumes were 37.55 and 32.76 cm^3/mol for CO_2 and air, respectively.

Shot	Impactor	u_I (km/s)	T_0 (K)	ρ_0 (g/cm^3)	u_s (km/s)	u_p (km/s)	P (GPa)[a]	V (cm^3/mol)
CO23	Al	4.928	218.8	1.171	6.609 ± 0.040	3.556 ± 0.021	27.52 ± 0.24	17.36 ± 0.18
CO22A	Al	6.451	218.4	1.172	7.912 ± 0.033	4.549 ± 0.026	42.19 ± 0.32	15.96 ± 0.16
CO21	Ta	5.143	218.5	1.172	8.645 ± 0.049	5.382 ± 0.038	54.53 ± 0.53	14.17 ± 0.23
CO24	Ta	6.070	218.5	1.172	9.646 ± 0.053	6.264 ± 0.049	70.82 ± 0.74	13.16 ± 0.25
AIR5	Al	5.706	77.1	0.884	7.442 ± 0.052	4.317 ± 0.025	28.40 ± 0.28	13.76 ± 0.18
AIR2	Ta	5.236	77.1	0.884	9.200 ± 0.138	5.788 ± 0.050	47.07 ± 0.80	12.15 ± 0.35
AIR4	Ta	6.752	77.1	0.884	10.56 ± 0.08	7.379 ± 0.062	68.86 ± 0.85	9.86 ± 0.28

[a] 1 GPa = 10 kbar.

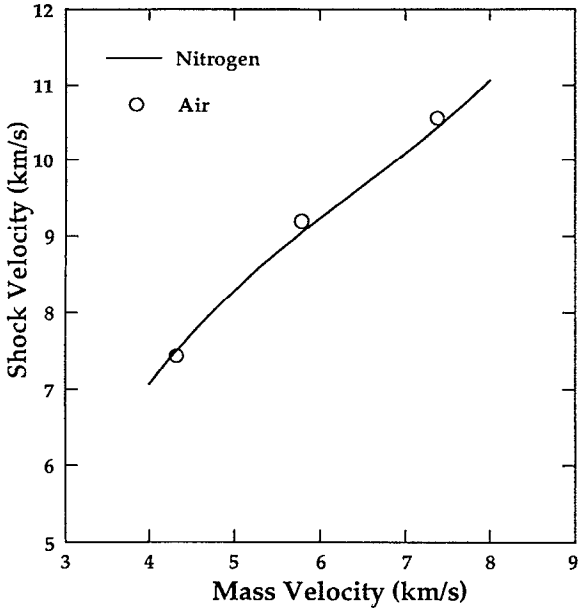

FIG. 2. Shock velocity vs mass velocity for liquid–air data (circles) and fit to liquid-nitrogen data (solid curve from Ref. 15).

included to allow some dissociated carbon atoms to precipitate under shock pressure. We minimize $G(P,T,\{n_i\})$ with respect to the compositions $\{n_i\}$ of the various species at fixed pressure P and temperature T. The resulting $G(P,T,\{n_i\})$ is used to compute thermodynamic quantities subject to the constraint of the Rankine–Hugoniot relations, Eqs. (1)–(3).

The minimization of the Gibb's free energy was carried out by the chemical equilibrium (CHEQ) code.[22] Briefly, for the condensed phases the code uses our three-phase model[23] of carbon which takes into account all relevant experimental and theoretical information on graphite, diamond, and liquid carbon. For gaseous mixtures it uses soft-sphere perturbation theory[24] and an improved mixture model[25] based on the van der Waals one-fluid theory. Our calculations employ the exponential-six (exp-6) potential with three parameters ϵ, r^*, and α. Since CO_2 is the dominant species in the present case, the discussion below will be concerned with the question of finding optimum parameter sets for CO_2. The CO parameters used in our calculations are described in Ref. 1 and those for O_2 and O are a slight modification of the parameters used in our earlier analysis of the shock data of liquid O_2.[3] The parameters for O_3 are estimated from the corresponding-states scaling relation with $\alpha = 13$.[26] A detailed theoretical account on the variation of the exp-6 parameters will be described in a separate paper.[27]

Our discussions are based on calculations with four sets of exp-6 parameters for CO_2:

Set A: $\epsilon/k = 245.6$ K, $r^* = 4.200$ Å, $\alpha = 13.5$,
Set B: $\epsilon/k = 335.0$ K, $r^* = 4.096$ Å, $\alpha = 13.5$,
Set C: $\epsilon/k = 335.0$ K, $r^* = 4.096$ Å, $\alpha = 13.78$,
Set D: $\epsilon/k = 245.6$ K, $r^* = 4.170$ Å, $\alpha = 13.5$,

where k is the Boltzmann constant. Sets A and D are our present modifications of an earlier parameter set[27] $(\epsilon/k, r^*, \alpha) = (245.6\text{ K}, 4.17\text{ Å}, 13)$, which was obtained by scaling the exp-6 parameters of argon.[28] Set D has a larger α (13.5) than the earlier set. Set A is made still stiffer by increasing r^*. Set C is that of Shaw and Johnson,[29] who modified their earlier set,[30] $(\epsilon/k, r^*, \alpha) = (338.3\text{ K}, 4.0935\text{ Å}, 14.400\ 25)$, to fit the data of Schott.[5]

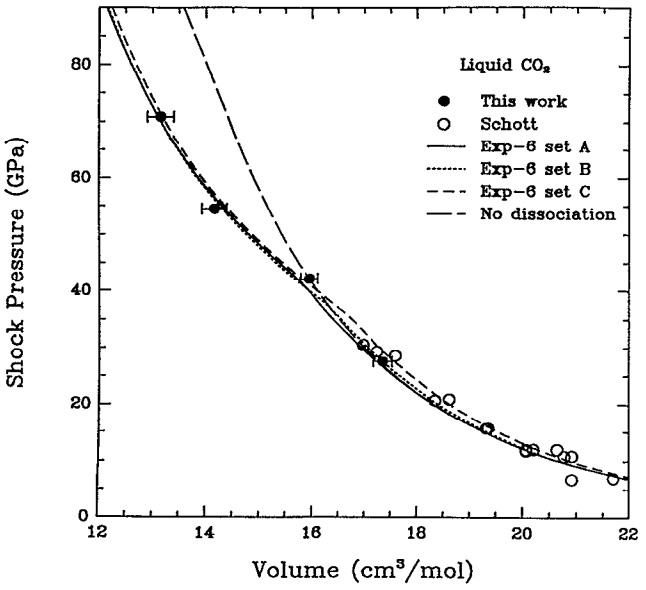

FIG. 3. Comparison of theoretical Hugoniots of CO_2 with experimental data of this work and with data of Ref. 5. Parameter sets are explained in text.

Figure 3 presents the P–V Hugoniots calculated from sets A, B, and C. They are compared with the experimental data in Sec. III and those of Schott. Set B has a lower α (13.5) than the value (13.78) used for set C. This was done to give a somewhat improved fit to the experimental data between 30 and 40 GPa. However, all these sets can be considered reasonable to 40 GPa. One important outcome from these calculations is that, at pressures above 40 GPa, a significant proportion of carbon atoms in CO_2 molecules will dissociate and condense into the liquid phase and that it gives rise to a shoulder-like structure seen in the experimental data near 40 GPa. If the CO_2 molecules are prohibited from the shock dissociation, the resulting Hugoniot will be much stiffer than the experimental data. Figure 3 includes such an example obtained from set A. Figure 4 shows the shock temperatures predicted from the parameter sets used in Fig. 3. As expected, the dissociation of CO_2 lowers considerably the shock temperature. Note that, in spite of sizable differences in values of ϵ and r^*, sets A and B both predict nearly identical shock pressure and temperature. This implies that, in selecting an optimum CO_2 potential to represent the conditions of interest here, other experimental data, such as double-shock data, are needed in addition to the single-shock data considered in this work.

It should be emphasized that the exp-6 potentials are effective two-body potentials, which spherically average the

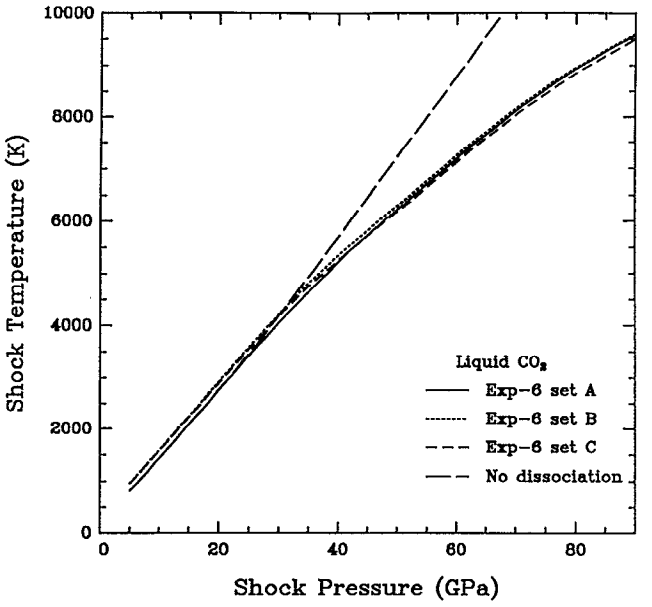

FIG. 4. Shock temperatures vs. shock pressures calculated with parameter sets used in Fig. 3.

angular dependence of molecular interactions. This approximation has been found to be adequate[30] for Hugoniot calculations at conditions such as those found in our experiments, where the temperatures are very high and comparable to or exceed the barriers to rotation.

In previous work which examined the shock data of simple molecules, such as Ar (Ref. 31) and He,[32,33] we found that the intermolecular potentials determined by fitting to the shock data and static high-pressure solid data were generally in good agreement. In Fig. 5 we made a similar test for CO_2. Set D described earlier fits to the 299.15 K solid isotherm data of Liu.[7] However, the same set produces a Hugoniot which is somewhat softer than the experimental shock data. On the other hand, set B which fits the experimental Hugoniot data predicts pressures higher than the solid isotherm above 15 GPa. Set A behaves similar to set B to ~30 GPa, beyond which it predicts slightly lower pressures. However, both sets A and B give pressures much higher than the experimental isotherm above 15 GPa. Set D, not shown, predicts even higher pressures. This is not surprising since CO_2 is a long linear molecule and the CO_2 molecules in the solid state at low temperatures and high pressures orient themselves in a geometry which minimizes their intermolecular repulsions. In comparison, high temperatures (Fig. 4) created by shock compression allow the CO_2 molecules to access some repulsive orientations, which are otherwise difficult under the low-temperature static environment of Liu's experiment. Thus, an effective spherical interaction (such as set A), which averages all orientations, will have too large a repulsion for low energy configurations, which in turn predicts pressures higher than the experimental solid isotherm.

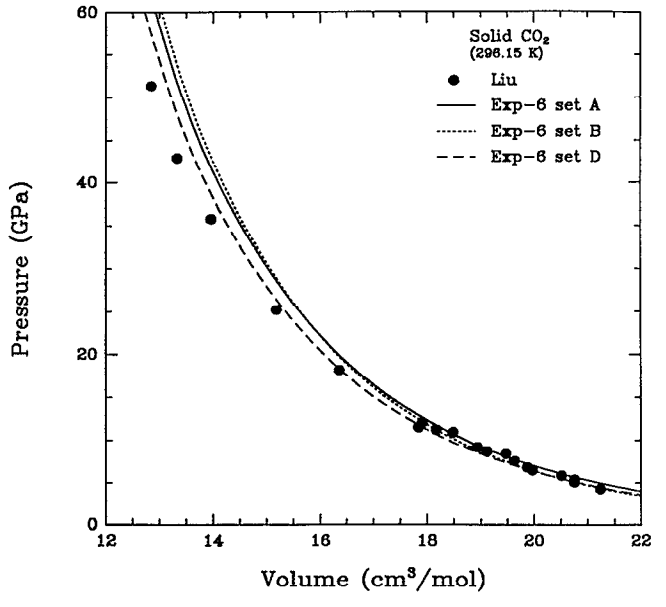

FIG. 5. Static isotherms of CO_2 at 299 K calculated using various exp-6 parameter sets compared with experimental data of Ref. 7.

ACKNOWLEDGMENTS

We acknowledge D. L. Ravizza and P. C. McCandless for fabricating the liquid-CO_2 specimen holders and gas-fill system, G. K. Governo for fabricating the liquid–air specimen holders, and K. C. Pederson, L. Oswald, and R. F. Schuldheisz for firing the two-stage light-gas gun. This work was performed under the auspices of the U. S. Department of Energy by the Lawrence Livermore National Laboratory under Contract No. W-7405-ENG-48.

[1] W. J. Nellis, F. H. Ree, M. van Thiel, and A. C. Mitchell, J. Chem. Phys. **75**, 3055 (1981).
[2] W. J. Nellis, N. C. Holmes, A. C. Mitchell, and M. van Thiel, Phys. Rev. Lett. **53**, 1661 (1984).
[3] D. C. Hamilton, W. J. Nellis, A. C. Mitchell, F. H. Ree, and M. van Thiel, J. Chem. Phys. **88**, 5042 (1988).
[4] V. N. Zubarev and G. S. Telegin, Sov. Phys. Dokl. 7, 34 (1962).
[5] G. L. Schott, High Press. Res. **6**, 187 (1991).
[6] B. Olinger, J. Chem. Phys. **77**, 6255 (1982).
[7] L. Liu, Earth Planet. Sci. Lett. **71**, 104 (1984).
[8] H. Olijnyk, H. Daufer, H.-J. Jodl, and H. D. Hochheimer, J. Chem. Phys. **88**, 4204 (1988).
[9] G. L. Schott, M. S. Shaw, and J. D. Johnson, J. Chem. Phys. **82**, 4264 (1985).
[10] H. B. Radousky, W. J. Nellis, M. Ross, D. C. Hamilton, and A. C. Mitchell, Phys. Rev. Lett. **57**, 2419 (1986).
[11] D. C. Hamilton and F. H. Ree, J. Chem. Phys. **90**, 4972 (1989).
[12] M. Ross, J. Chem. Phys. **86**, 7110 (1987).
[13] A. C. Mitchell and W. J. Nellis, Rev. Sci. Instrum. **52**, 347 (1981).
[14] W. J. Nellis and A. C. Mitchell, J. Chem. Phys. **73**, 6137 (1980).
[15] W. J. Nellis, H. B. Radousky, D. C. Hamilton, A. C. Mitchell, N. C. Holmes, K. B. Christianson, and M. van Thiel, J. Chem. Phys. **94**, 2244 (1991).
[16] A. C. Mitchell and W. J. Nellis, J. Chem. Phys. **76**, 6273 (1982).
[17] *International Thermodynamic Tables of the Fluid State: Carbon Dioxide*, edited by S. Angus, B. Armstrong, and K. M. de Reuck (Pergamon, Oxford, 1976), p. 78.
[18] N. B. Vargaftik, *Tables on the Thermophysical Properties of Liquids and Gases*, 2nd ed. (Hemisphere, Washington, 1975), p. 586.
[19] A. C. Mitchell and W. J. Nellis, J. Appl. Phys. **52**, 3363 (1981).
[20] N. C. Holmes, J. A. Moriarty, G. R. Gathers, and W. J. Nellis, J. Appl. Phys. **66**, 2962 (1989).
[21] R. D. Dick, J. Chem. Phys. **52**, 6021 (1970).

[22] (a) F. H. Ree, J. Chem. Phys. **81**, 1251 (1984); (b) **84**, 5845 (1986).
[23] (a) M. van Thiel and F. H. Ree, Int. J. Thermophys. **10**, 227 (1989); (b) M. van Thiel and F. H. Ree (in preparation). The present calculations used a slightly different value (i.e., 0 instead of 0.1) for d_{1c} in Table I, Ref. 23(a). This parameter is one the parameters used to describe the thermal correction to the Helmholtz free energy of graphite.
[24] M. Ross, J. Chem. Phys. **73**, 4445 (1980).
[25] M. Ree, J. Chem. Phys. **78**, 409 (1983).
[26] M. Ross and F. H. Ree, J. Chem. Phys. **73**, 6146 (1980).
[27] F. H. Ree and M. van Thiel (in preparation).
[28] M. Ross, J. Chem. Phys. **73**, 4445 (1980).
[29] M. S. Shaw and J. D. Johnson, in *Proceedings of the Eighth Symposium (International) on Detonation*, edited by J. M. Short, NSWC-MP-86-194 (Naval Surface Weapons Center, White Oak, MD, 1986), p. 531.
[30] J. D. Johnson and M. S. Shaw, J. Chem. Phys. **83**, 1271 (1985).
[31] M. Ross, H. K. Mao, P. M. Bell, and J. A. Xu, J. Chem. Phys. **85**, 1028 (1986).
[32] M. Ross and D. A. Young, Phys. Lett. A **118**, 463 (1986).
[33] H. K. Mao, R. J. Hemley, Y. Wu, A. P. Jephcoat, L. W. Finger, C. S. Zha, and W. A. Bassett, Phys. Rev. Lett. **60**, 2649 (1988).